4. V. J. Puglisi and A. J. Bard, *ibid.*, **119**, 829 (1972).
5. E. Lamy, L. Nadjo, and J. M. Saveant, *J. Electroanal. Chem.*, **42**, 189 (1973).
6. J. W. Ross, R. D. DeMars, and I. Shain, *Anal. Chem.*, **28**, 1768 (1956).
7. P. Delahay, C. C. Mattax, and T. Berzins, *J. Am. Chem. Soc.*, **76**, 5319 (1954).
8. T. Berzins and P. Delahay, *ibid.*, **75**, 4205 (1953).
9. O. Dracka, *Collection Czech. Chem. Commun.*, **25**, 338 (1960).
10. A. C. Testa and W. H. Reinmuth, *Anal. Chem.*, **32**, 1512 (1960).
11. S. W. Feldberg, in "Electroanalytical Chemistry," Vol. 3, A. J. Bard, Editor, pp. 199-296, Marcel Dekker, Inc., New York (1969).
12. S. W. Feldberg and M. D. Hawley, *J. Phys. Chem.*, **70**, 3459 (1966).
13. W. H. Reinmuth, *Anal. Chem.*, **33**, 485 (1961).
14. M. L. Olmstead, R. G. Hamilton, and R. S. Nicholson, *ibid.*, **41**, 260 (1969).

Chronopotentiometric Investigation of the Oxidation of Aluminum in Chloroaluminate Melts

B. Gilbert,[1] D. L. Brotherton, and G. Mamantov*

Department of Chemistry, University of Tennessee, Knoxville, Tennessee 37916

ABSTRACT

Oxidation of an aluminum electrode in molten $AlCl_3$-MCl (63-37 mole per cent, M = Na or Li) has been investigated by chronopotentiometry. Well-defined and reproducible transition times, caused by the formation of a poorly conducting Al_2Cl_6 layer at the electrode surface and the depletion of current-carrying alkali metal ions, were observed. The observations are in very good agreement with the theoretical predictions similar to those of Braunstein and co-workers. In the range of current densities employed (up to 300 mA/cm^2 at 140°C), the aluminum electrode behaves reversibly.

It has been very recently shown by Braunstein and co-workers (1) that in molten alkali metal fluoride-beryllium fluoride mixtures, the chronopotentiometric oxidation of a beryllium anode results in a layer of nearly pure, almost nonconductive BeF_2 as the mobile alkali metal ions are swept away, and, as the result, the potential of the beryllium anode rises sharply.

The important feature of this phenomena is that the boundary conditions of the diffusion law are not determined by depletion of an electroactive constituent but by migration of the mobile nonelectroactive alkali metal ion. A theoretical treatment based on the concentration cell principle was developed to explain the observed chronopotentiograms.

An aluminum electrode in molten $AlCl_3$-MCl (M-alkali metal ion) melts should exhibit similar behavior. Holleck and Giner (2) have observed passivation phenomena in the anodic oxidation of an Al electrode in $AlCl_3$-KCl-NaCl melts between 100° and 160°C. The phenomena were attributed to the formation of a solid salt layer at the electrode surface, resulting from concentration changes upon current flow.

We were interested in exploring quantitatively the anodization of an Al electrode by applying the theory developed by Braunstein (1). Besides being of fundamental interest, the results of such a study are clearly of importance to the use of Al anodes in chloroaluminate melts, for example, in battery applications (3).

Experimental

The electrochemical cell, instrumentation, and procedure have been described previously (4, 5). An aluminum wire (m5N from Alfa Inorganics) immersed in molten $AlCl_3$-MCl [63-37 mole per cent (m/o)] was used as the working electrode (surface area ≃0.1 cm^2). The reference electrode was an aluminum wire (m5N) immersed in the same melt composition and separated from the main compartment by a thin Pyrex membrane. A platinum wire electrode was used to check the purity of the melt by cyclic voltammetry.

Each melt was clear and waterlike at the beginning of each experiment. After several days, the melt became slightly brown and frequently the Al electrode was covered with a black deposit, possibly a layer of aluminum metal-rich alumina caused by oxyanions coming from the Pyrex glass (6). At this point, the measurements were no longer reproducible and were not included.

Basic Relationships

The controlled current oxidation of an Al electrode increases the concentration of $AlCl_3$ (more correctly Al_2Cl_6) in the vicinity of the electrode and the reversible emf should correspond to the resulting concentration cell

$$\mathrm{Al} \;\Big|\; \begin{matrix}\mathrm{AlCl_3\text{-}MCl} \\ y_o\end{matrix} \;\Big\vert\; \begin{matrix}\mathrm{AlCl_3\text{-}MCl} \\ y = y_o + \Delta y\end{matrix} \;\Big|\; \mathrm{Al}$$

Such a cell should exhibit an emf corresponding to (1, 7)

$$E = \frac{1}{3F}\int_{y_o}^{y}(1 - t_{Al^{3+}})\left(\frac{1+2y}{1-y}\right)\frac{d\mu_{AlCl_3}}{dy}\,dy \quad [1]$$

where y and μ are the stoichiometric mole fraction and chemical potential of $AlCl_3$, respectively, y_o is the initial stoichiometric mole fraction of $AlCl_3$, and $t_{Al^{3+}}$ is the transference number of Al^{3+}.

If we assume that the transference number of Al^{3+} is essentially zero, the only current carrying species (relative to chloride) is the alkali metal cation and the emf becomes

$$E = \frac{RT}{3F}\left[\ln\frac{y}{(1-y)^3} - \ln\frac{y_o}{(1-y_o)^3} + \int_{y_o}^{y}\left(\frac{1+2y}{1-y}\right)\frac{d\ln\gamma_{AlCl_3}}{dy}\,dy\right] \quad [2]$$

where γ is the activity coefficient of $AlCl_3$ corresponding to above concentration units. The standard state in this case is similar to that employed by Hitch and Baes (8) and corresponds to pure molten $AlCl_3$.

* Electrochemical Society Active Member.
[1] Permanent address: University of Liege, Belgium.
Key words: molten halides, molten chloroaluminates, chronopotentiometry, aluminum oxidation in melts.

The first two terms in Eq. [2] give the ideal emf; the third term corresponds to the "excess" emf which may be calculated if the variation of the activity coefficient with stoichiometric mole fraction is known.

Similar equations can be developed for other systems, and, in general, for a system $M + nX^- \underset{}{\overset{-ne^-}{\rightleftharpoons}} MX_n$, the emf is given by

$$E = \frac{1}{nF}\int_{y_o}^{y}(1 - t_{Mn+})\left[\frac{1 + (n-1)y}{1-y}\right]\frac{d\mu_{MX_n}}{dy}\,dy \qquad [3]$$

which gives, if $t_{Mn+} = 0$

$$E = \frac{RT}{nF}\left\{\ln\frac{y}{(1-y)^n} - \ln\frac{y_o}{(1-y_o)^n} + \int_{y_o}^{y}\left[\frac{1 + (n-1)y}{1-y}\right]\frac{d\ln\gamma_{MX_n}}{dy}\,dy\right\} \qquad [4]$$

Thus, the emf of the cell does not follow the usual Nernst type behavior. However, as shown previously (1), it is possible to obtain the variation of concentrations of MCl and $AlCl_3$ at the electrode surface with time from the solution of the diffusion equation for ordinary chronopotentiometry. These quantities can be substituted into Eq. [2], as shown below, to obtain the variation of cell emf with time, and, thus, the chronopotentiogram. Sand's equation (9) should be applicable (1).

Results

To obtain well-defined and reproducible chronopotentiograms it was necessary to set the potential of the aluminum electrode to the initial equilibrium potential after each chronopotentiogram. In order to get reasonable transition times, high (~200°C) and low (~120°C) temperatures must be avoided. At these temperature extremes the transition times are either much too long (several minutes) or too short (the passivating layer forms very quickly), respectively. If the above conditions are followed, the reproducibility of transition times is better than 5%.

Typical chronopotentiograms are shown in Fig. 1. The potential of the aluminum electrode was corrected for the initial *IR* drop. The applicability of Sand's equation is shown in Fig. 2. Each point is an average of 5-8 measurements. The constancy of the product $i\tau^{1/2}$ shows clearly that in the range investigated, the oxidation process is controlled by diffusion. This conclusion supports the results of Holleck, obtained from measurements of the anodic limiting current of a rotating aluminum electrode (2).

The "ideal" emf in Eq. [2] expressed in terms of equivalent concentrations, becomes

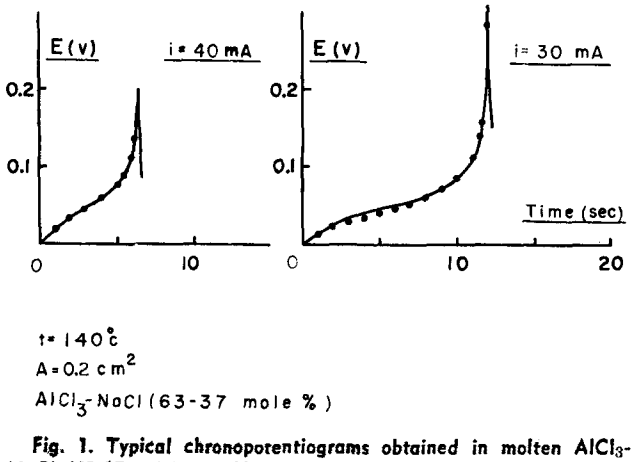

Fig. 1. Typical chronopotentiograms obtained in molten $AlCl_3$-NaCl (63-37 m/o) at 140°C. The points correspond to the calculated curve based on an ideal behavior (Eq. [5]). The experimental curves were corrected for the *IR* drop. The applied currents are 40 and 30 mA, respectively; $A = 0.2$ cm²; $t = 140$°C.

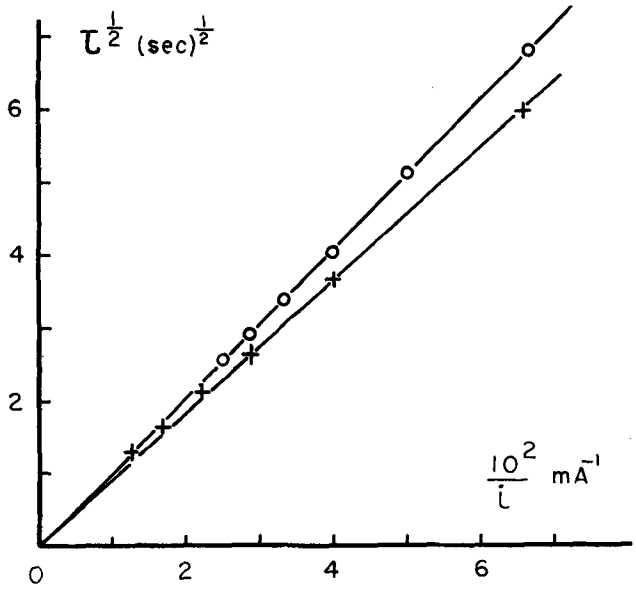

Fig. 2. Plot of $\tau^{1/2}$ vs. $1/i$ for the system $AlCl_3$-NaCl (63-37 m/o). ○, $t = 140$°C; ×, $t = 130$°C.

$$\frac{3FE^{ideal}}{RT} = \ln\left\{\frac{[1 - C_{NaCl}\bar{V}_{NaCl}][1 + (\bar{V}_{AlCl_3} - \bar{V}_{NaCl})C_{NaCl}]^2}{[\bar{V}_{AlCl_3}C_{NaCl}]^3}\right\} - \ln\left\{\frac{[1 - C^o_{NaCl}\bar{V}_{NaCl}][1 + (\bar{V}_{AlCl_3} - \bar{V}_{NaCl})C^o_{NaCl}]^2}{[\bar{V}_{AlCl_3}C^o_{NaCl}]^3}\right\} \qquad [5]$$

where C^o and C are the initial and instantaneous concentrations (expressed in equivalents/cm³) (1) and $\bar{V}$ is the partial molal volume.

The above equation can be solved knowing that at any time we must have

$$C_{Na+} = C^o_{Na+} - \alpha t^{1/2} \qquad [6]$$

where

$$\alpha = \frac{2i}{\pi^{1/2}D^{1/2}AnF} \qquad [7]$$

and

$$C_{Na+} = C_{NaCl}$$

For $t = \tau$, we have a pure layer of $AlCl_3$ (Al_2Cl_6) at the electrode surface and $C_{NaCl} = 0$, so $\alpha\tau^{1/2} = C^o_{NaCl}$. C^o_{NaCl} is estimated from the densities of the melt at the investigated temperatures and the stoichiometric mole fractions of NaCl and $AlCl_3$. The densities of the melt were extrapolated from the work of Boston (10).

For $AlCl_3$-NaCl (63-37 m/o), C^o_{NaCl} is 0.00585 equiv/cm³ at 140°C. From this value and Fig. 2, we can determine α and the average interdiffusion coefficient D. D was found to be 1×10^{-6} cm²/sec at 140°C. A value of D of this order of magnitude is not unreasonable considering that the transport process involves the diffusion of Na^+ ions in $AlCl_3$-rich melts; the composition of the melt at the electrode changes continuously during the chronopotentiogram from the initial composition (63 m/o $AlCl_3$) to essentially pure Al_2Cl_6. We have previously reported (11) the diffusion coefficient for Ti(II) in $AlCl_3$-NaCl (65-35 m/o) to be in the range $2.5\text{-}6 \times 10^{-6}$ cm²/sec at temperatures 185°-260°. The diffusion coefficient for Ti(III) in LiF-BeF_2-ZrF_4 (65.6-29.4-5.0 m/o) at 500°C was found to be 1.0×10^{-6} cm²/sec (12). Lower values of D would be expected in viscous BeF_2-rich mixtures. From the above comparison, a higher value of D for Na^+ in acidic chloroaluminates used in this work would be expected compared to the value of D of 3×10^{-7}

cm²/sec obtained by Braunstein *et al* (1) for the diffusion of Na^+ in BeF_2-NaF (75-25 m/o) at 520°C.

If we make the assumption that the diffusion coefficient is constant as the concentration changes, we can calculate C_{NaCl} as a function of time from Eq. [6] and from that the ideal emf. It was assumed in this calculation that the partial molal volumes are additive; this assumption is only approximately correct for this system (10).

Calculated points are also given in Fig. 1. The "ideal" curve is in reasonable agreement with the experimental curve; however, the calculated points lie slightly below the experimental values except in the final part of the curve. It can also be seen that the calculated curve fits the experimental curve better if the transition time is short.

In our calculation, D was assumed to remain constant as the composition changes (not a correct assumption). Furthermore, for the system $AlCl_3$-NaCl it has been observed (13-15) that above 80 m/o of $AlCl_3$ and above 193°C, two liquid phases occur, of which one is probably almost pure Al_2Cl_6. Hence the point where a pure layer of Al_2Cl_6 is formed at the electrode should occur sooner than in the absence of two liquid phases. The time for which $y = 0.80$ can be easily calculated from Eq. [6] and one obtains in general that $t_{y=0.80} = 0.26\tau$. Thus, if the observed transition time corresponds to the immiscibility, the true transition time is about four times longer. For this condition, the calculated curve exhibits a very flat region with a sudden potential increase when the immiscibility occurs. At this point the concentration of Na^+ ions at the electrode surface is zero. The shape of the calculated chronopotentiogram would be different from what we observed. Nevertheless, in the range of our working temperatures, the pure Al_2Cl_6 produced at the end of the chronopotentiogram, or in the region of immiscibility, should be a solid. Such a solid layer can be easily observed on the electrode for temperatures lower than 120°C and also at very long transition times. If this is the case, the measurements are no longer reproducible. For temperatures between 130° and 160°C, the solid phase is not observed except if the transition time exceeds several minutes. Under these conditions, the results suggest that the melt is supersaturated with Al_2Cl_6 in the vicinity of the electrode, as also noted by Holleck and Giner (2).

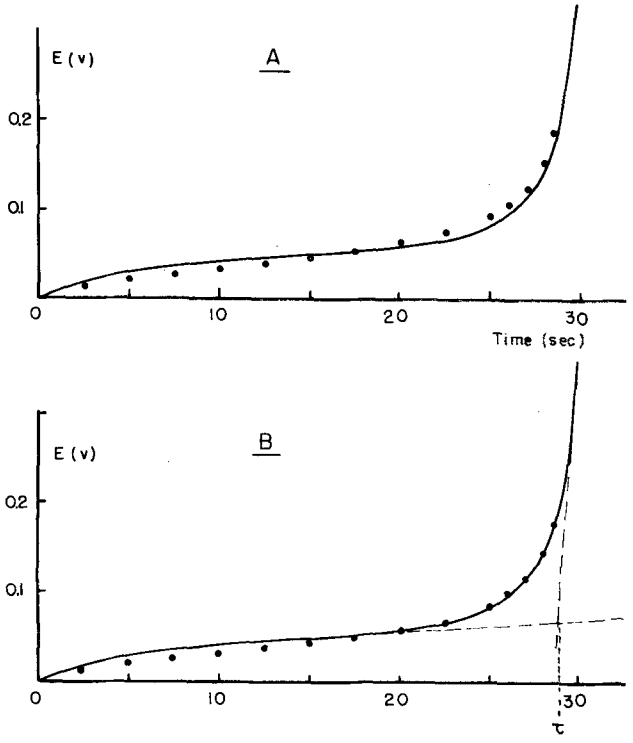

Fig. 3. Chronopotentiogram obtained in molten $AlCl_3$-LiCl (63-37 m/o); $t = 150$°C; $i = 25$ mA; $A = 0.13$ cm². The points are calculated from Eq. [5] for curve A and from Eq. [5] + [11] for curve B.

In the case of $AlCl_3$-LiCl, no immiscibility has been reported in the literature, although the only paper reporting the phase diagram of this system is rather old (13). The experimental and calculated chronopotentiograms for $AlCl_3$-LiCl (63-37 m/o) are given in Fig. 3.

A negative deviation in the first part of the theoretical curve and a slight positive deviation for the second half of the curve are observed. The latter observation depends mostly on the chosen value of the transition time τ. τ was determined by the method of Reinmuth (16). The corresponding average interdiffusion coefficient is 4.5×10^{-6} cm² sec^{-1}, higher than for the NaCl system as might be expected from the smaller size of the lithium cation.

Over-all, the shape of the experimental curve is only slightly different than for the $AlCl_3$-NaCl system and also fits the theoretically calculated curve. This indicates that the immiscibility did not have time to develop in the case of $AlCl_3$-NaCl.

The preceding calculations deal only with ideal emf. In order to calculate the effect of the "excess" emf, the variation of the activity coefficients with composition must be known. Fannin and co-workers (7) have proposed a least squares empirical polynomial for $d \ln \gamma/dy$ in which the activity coefficients are calculated from vapor pressure measurements. In this case, the excess function becomes

$$E^{excess} = \frac{RT}{3F} \int_{y_o}^{y} (1 - t_{Al3+}) \left(\frac{1 + 2y}{1 - y} \right) (C_1 + 2C_2 y + 3C_3 y^2)\, dy \quad [8]$$

However, the values of the coefficients C_1, C_2, and C_3 are not given; in any case, this polynomial was determined only in the range 0.55-0.75 mole fraction of $AlCl_3$. In view of the fact that no experimental data are available for the very acidic melts, we have used a very simple function based on the assumption that the melt behaves as a regular solution (17). This assumption is not correct due to strong interactions between the melt constituents; however, it is interesting to know in what way a correction for the activity coefficients will affect the ideal function even if this correction is very approximate. Thus the activity coefficients were estimated from (17)

$$RT \ln \gamma = w(1 - y)^2 \quad [9]$$

where w is a constant.

The excess emf then becomes

$$E^{excess} = \frac{w}{3F} \int_{y_o}^{y} (1 - t_{Al3+}) \left(\frac{1 + 2y}{1 - y} \right) (2y - 2)\, dy \quad [10]$$

This equation contains only one adjustable parameter, w. Comparison of Eq. [10] with Eq. [8] shows that the third term in Eq. [8] ($3C_3y^2$) has been neglected and the constants are related by $C_2 = -C_1/2 = w/RT$; however, there are no basic differences between the two equations.

After integration of Eq. [10] and expressing y as a function of C_{NaCl}, we obtain

$$E^{excess} = \frac{2w}{3F} \left\{ - \frac{(1 - C_{NaCl}\bar{V}_{NaCl})[2 + (\bar{V}_{AlCl_3} - 2\bar{V}_{NaCl})C_{NaCl}]}{[1 + (\bar{V}_{AlCl_3} - \bar{V}_{NaCl})C_{NaCl}]^2} + \frac{(1 - C^o_{NaCl}\bar{V}_{NaCl})[2 + (\bar{V}_{AlCl_3} - 2\bar{V}_{NaCl})C^o_{NaCl}]}{[1 + (\bar{V}_{AlCl_3} - \bar{V}_{NaCl})C^o_{NaCl}]^2} \right\} \quad [11]$$

Since the absolute value of the first term in the parenthesis is always larger than that of the second, the value of the parenthesis is negative and the sign of the excess function is thus opposite to the sign of the constant w. It is also worth noting that this approximate function giving E^{excess} affects mostly the end of the chronopotentiogram; this result is similar to that obtained by Braunstein *et al.* (1) An average value of $w \simeq 7 \times 10^2$ j-mole^{-1} has been calculated to fit the experimental curve for the system $AlCl_3$-LiCl. The final result is given in curve B of Fig. 3 for which the agreement between the calculated and experimental values is quite good, particularly considering the approximations involved.

Conclusions

Excellent agreement between theory and experiment has been obtained for the anodic oxidation of Al in $AlCl_3$-NaCl (63-37 m/o) and in $AlCl_3$-LiCl (63-37 m/o). It is clear that the mechanism resulting in the chronopotentiogram (formation of a poorly conducting Al_2Cl_6 layer at the electrode surface and the depletion of current carrying alkali metal ions) is analogous to that observed for MF-BeF_2 mixtures (1). Since the calculated curves are obtained from assuming a reversible concentration cell, the observed agreement shows that the Al electrode behaves reversibly in the range of current densities employed. Furthermore, the applicability of Sand's equation requires that the oxidation process is diffusion controlled.

Acknowledgments

This work was supported by the National Science Foundation under Contract NSF GP 32433X. A grant-in-aid from ALCOA Foundation is also gratefully acknowledged. The authors are pleased to acknowledge useful discussions with Drs. Jerry Braunstein and Catherine Vallet.

Dr. Gilbert has received partial support from the Fonds National de la Recherche Scientifique of Belgium.

Manuscript submitted Oct. 26, 1973; revised manuscript received Feb. 5, 1974.

Any discussion of this paper will appear in a Discussion Section to be published in the December 1974 JOURNAL. All discussions for the December 1974 Discussion Section should be submitted by Aug. 1, 1974.

REFERENCES

1. J. Braunstein, H. R. Bronstein, and J. Truitt, *J. Electroanal. Chem.*, **44**, 463 (1973).
2. G. L. Holleck and J. Giner, *This Journal*, **119**, 1161 (1972).
3. G. D. Brabson, A. A. Fannin, Jr., L. A. King, and D. W. Seegmiller, Abstract 26, p. 61, Electrochemical Society Extended Abstracts, Spring Meeting, Chicago, Illinois, May 13-18, 1973.
4. G. Torsi, K. W. Fung, G. M. Begun, and G. Mamantov, *Inorg. Chem.*, **10**, 2285 (1971).
5. G. Torsi and G. Mamantov, *J. Electroanal. Chem.*, **30**, 193 (1971).
6. G. F. Uhlig, Dissertation, University of Utah, 1973.
7. A. A. Fannin, Jr., L. A. King, and D. W. Seegmiller, *This Journal*, **119**, 801 (1972).
8. B. F. Hitch and C. F. Baes, Jr., *Inorg. Chem.*, **8**, 201 (1969).
9. P. Delahay, "New Instrumental Methods in Electrochemistry," p. 184, Interscience Publishers, New York (1954).
10. C. R. Boston, *J. Chem. Eng. Data*, **11**, 262 (1966).
11. K. W. Fung and G. Mamantov, *J. Electroanal. Chem.*, **35**, 27 (1972).
12. F. R. Clayton, G. Mamantov, and D. L. Manning, *This Journal*, **120**, 1193 (1973).
13. J. Kendall, E. D. Crittenden, and H. K. Miller, *J. Am. Chem. Soc.*, **45**, 963 (1923).
14. U. I. Shvartsman, *J. Phys. Chem. (USSR)*, **14**, 253 (1940).
15. V. W. Fischer and A.-L. Simon, *Z. Anorg. Allgem. Chem.*, **306**, 1 (1960).
16. W. H. Reinmuth, *Anal. Chem.*, **33**, 485 (1961).
17. L. G. Boxall, H. L. Jones, and R. A. Osteryoung, *This Journal*, **120**, 223 (1973).

Brief Communication

Electrodeposition of an Amorphous Cobalt Rhenium Alloy

P. J. Cote, G. P. Capsimalis, and V. P. Greco

Watervliet Arsenal, Watervliet, New York 12189

The publication costs of this article have been assisted by the Department of the Army.

We are reporting on the formation of a cobalt-44 atomic per cent (a/o) rhenium amorphous alloy by electrodeposition from a bath developed by Netherton and Holt (1). The bath composition used to obtain the amorphous phase is given in Table I.

Our fabrication of a new amorphous metal is significant in view of the current interest in these materials and the fact that relatively few amorphous alloys have been electrodeposited.

Both x-ray and electron diffraction patterns show the diffuse rings which are characteristic of these materials (see Fig. 1).

Electrodeposition studies were made using the Beckman "Electroscan 30." Current density *vs.* cathode potential scans were obtained in the potentiostatic mode and these revealed a break at around −850 mV as shown in Fig. 2. These data were taken in a quiescent bath. The break is far less pronounced in the stirred baths in which the specimens were prepared. Deposits made above the break generally result in the amor-

Key words: amorphous, electrodeposition, cobalt-rhenium alloy.

Table I.

Bath formula	Concentration (g/liter)
$CoSO_4$ $7H_2O$	60
Citric acid	66
NH_4ReO_4	4
pH	7.6